

Voltage Hash of Various Propellants in Self-Field Magnetoplasmadynamic Thrusters

IEPC-2009-230

*Presented at the 31st International Electric Propulsion Conference,
University of Michigan, Ann Arbor, Michigan, USA
September 20–24, 2009*

Daisuke Nakata*

Japan Aerospace Exploration Agency, 3-1-1, Yoshinodai, Sagamihara-shi, Kanagawa 229-8510, Japan

Kyoichiro Toki†

Tokyo University of Agriculture and Technology, 2-24-16, Nakacho, Koganei-shi, Tokyo 184-8588, Japan

Yukio Shimizu‡

Japan Aerospace Exploration Agency, 3-1-1, Yoshinodai, Sagamihara-shi, Kanagawa 229-8510, Japan

and

Hitoshi Kuninaka§

Japan Aerospace Exploration Agency, 3-1-1, Yoshinodai, Sagamihara-shi, Kanagawa 229-8510, Japan

Abstract: It is well known phenomena called “ Onset ” that the drastic voltage fluctuation and anode erosion occurs above the threshold current. This threshold current is considered to be inversely proportional to the molecular mass of the propellant, but the molecular gases such as hydrogen does not follow this tendency whereas it is well confirmed for atomic gases. It is well known that some voltage fluctuation is always recognized even in small discharge current in the case of hydrogen. In this study, voltage waveforms of argon, hydrogen and xenon were experimentally obtained with careful attention, and compared. For argon and xenon, the amplitude of the voltage fluctuation is getting larger with increasing discharge current. Its peak-spectrum frequency was in several hundreds of kHz. For hydrogen, the amplitude and the peak-spectrum frequency of the voltage fluctuation was almost constant regardless of the discharge current.

Nomenclature

f_{peak}	=	peak frequency in discharge voltage spectrum
J	=	discharge current
\dot{m}	=	mass flow rate
V	=	discharge voltage
ΔV	=	amplitude of discharge voltage fluctuation

*Researcher, Japan Space Exploration Center, E-mail: nakata@ep.isas.jaxa.jp

†The late Professor, Department of Mechanical System Engineering, E-mail: toki@cc.tuat.ac.jp

‡Research Engineer, Space Transportation Division, E-mail: shimizu@isas.jaxa.jp

§Professor, Space Transportation Division, E-mail: kuninaka@isas.jaxa.jp

I. Introduction

It is well known that the propulsive efficiency of a magnetoplasmadynamic thruster (MPDT) is monotonically increasing with J^2/\dot{m} . However, when the value of J^2/\dot{m} exceeds the critical value $(J^2/\dot{m})_{crit.}$, drastic voltage fluctuation and severe electrode damage is observed. Due to this phenomena, it is not allowed to increase J^2/\dot{m} arbitrary.

The maximum practical efficiencies for various propellants obtained in MPD experiments in the world are shown in Table 1, which is arranged by Choueiri.¹ This is defined at the "onset threshold point" of each propellant. However, it is generally very difficult to define the "onset threshold point" in the case of hydrogen, which gives the highest efficiency among all of propellants. Many researchers might experience that the voltage fluctuation of hydrogen is almost always observed regardless of its operational condition. Fischer² pointed out the amplitude of the voltage fluctuation ΔV in the case of hydrogen decreased with J^2/\dot{m} at first, and increases above $J^2/\dot{m} = 10^{11}$ A²s/kg.

This intrinsic tendency impedes to know the practical operational limit of MPDT with hydrogen propellant. In 1980s, the operational characteristics of MPDT with various propellants (H₂, CH₄, NH₃, H₂O, CO₂, CO, O₂, N₂, He, Ne, Ar, Xe) were examined by Uematsu,³ but he used filter passing frequencies below about 40 kHz due to eliminate the ambiguity when determining the mean terminal voltage. So the maximum practical efficiency is still ambiguous in his enormous data set. He knew that the voltage fluctuation was always observed especially in case of hydrogenous gases. In the series of steady-state mode experiment performed in Stuttgart University, the voltage fluctuation was observed from very small (J^2/\dot{m}) in the case of hydrogen. Therefore, the attention has not been paid to hydrogen in their steady-state MPDT experiment.

For practical reason, it is very important to know the exact threshold point in case of hydrogen. In smaller (J^2/\dot{m}), the anode erosion does not seem severe. The origin of the voltage fluctuation is often explained by the lack of the electric career near the anode,⁴ but the background which causes the voltage fluctuation in the case of hydrogen at small (J^2/\dot{m}) might be different.

In this study, we will not give any conclusive answer to this problem, but will provide the informative suggestion based on the experimental data of argon, xenon and hydrogen as propellants. One can understand the macroscopic feature of voltage fluctuation clearly by seeing raw voltage waveforms displayed in this paper.

Table 1. Maximum practical efficiency (at the "Onset threthold point") in an MPD thruster¹ .

propellant	efficiency
H ₂	55 %
NH ₃	35 %
N ₂	38 %
He	20 %
Ar	30 %

II. Experimental Apparatus

The experimental apparatus and the procedure adopted in this study are almost similar to our past MPDT studies.^{5,6} A schematic of the thruster is shown in Fig. 1. In this "Straight" configuration, it is considered that the arc current generally strikes on the side surface of the cathode, especially on the root of the cathode rather than the cathode tip. The cylindrical-shape anode is made of phosphor bronze and its inner and outer diameter is 28 mm and 80 mm, respectively. Sintered tungsten cathode (2 % ThO₂-W) 42 mm in length and 8 mm in diameter, ending in a hemispherical tip is pressed into the phosphor bronze holder. The thruster is set in a stainless steel-vacuum tank 2.0-m long and 0.92-m in diameter. Tank pressure is maintained to less than 7 mPa prior to each firing. Gaseous argon propellant is injected through eight choke orifices of fast-acting valves (FAV) for 5 ms in rectangular waveform. The mass flow rate at their steady-state values is 0.8 g/s with 5 % of shot-to-shot variation. The discharge current supplied by a pulse-forming network (PFN) with an energy storage capability of 25 kJ forms a rectangular waveform of 0.45-ms. The discharge current is measured by a Rogowski coil, and the discharge voltage is monitored by sensing the small current through a shunt resistor (100 Ω) connected between the anode and the cathode.

Yokogawa 700937 current probe (which can detect the signal up to 500 MHz) and Yokogawa DL9000 (up to 2GW/s sampling is possible) digital oscillo scope were used for detecting the small current. This divider line was attached to the closest point (rear surface of the thruster head) as possible in order to avoid the transmission line resonance.⁷ Besides, the characteristic frequency was measured by LCR tester as shown in Table 2.

Table 2. .The electrical characteristics of divided line.

L	5 μ H
C	300 pF
R	101.9 Ω
f_{res}	4 MHz

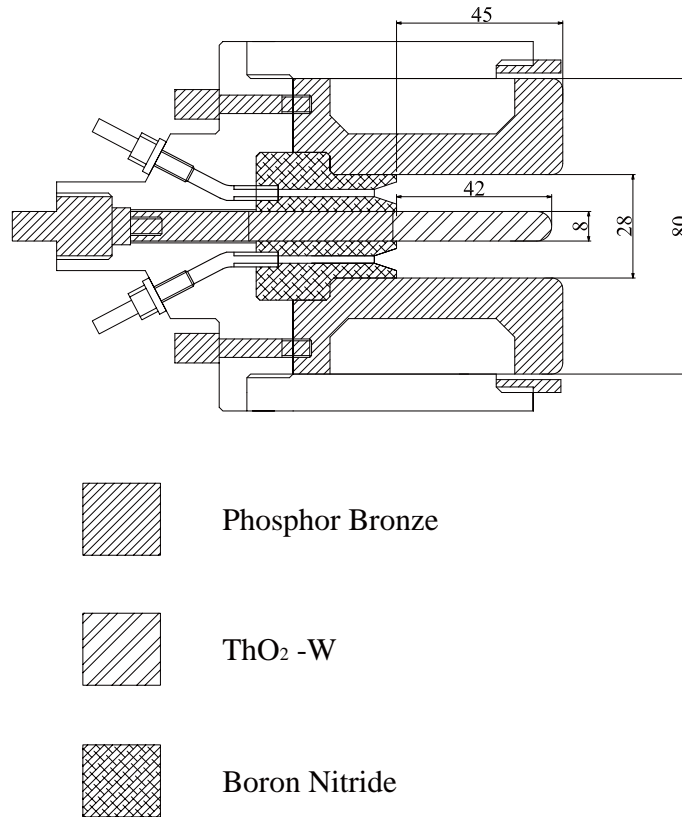


Figure 1. Cross sectional view of the MPD thruster. (Straight configuration)

III. Experimental Results

In this study, argon, hydrogen and xenon were selected as propellants. The mass flow rate of each propellant is shown in Fig. 3. Since the molecular weight of xenon is 3.3 times larger than that of argon, the mass flow rate is set at $\sqrt{3.3}$ times larger than that of argon. To do so, it is considered that the transition from stable to unstable voltage waveform can be observed in same range of discharge current ($J = 5-15$ kA). Similarly, the mass flow rate of hydrogen should be set at $1/\sqrt{40} \simeq 0.13g/s$, but the ignition did not occur successfully at this mass flow rate. So, we used much larger mass flow rate which gave firm ignition. Figure 2 is the discharge voltage(i.e. terminal voltage) vs. the discharge current characteristics for each propellant. Almost quadratically increasing feature of the voltage is recognized for argon and xenon. On the other hand, voltage curve of hydrogen shows almost linear to the discharge current. This implies

that the energy consumption is mainly due to joule heating rather than back EMF.

The data set are shown in Figs 3- 8. In each figure, raw data (left), magnified views (upper right) and the FFT spectra (lower right) of voltage waveforms are displayed. The terminal voltage is determined by the mean value between the two dashed vertical line appeared in raw voltage waveform. FFT analysis is also done in this region. In order to avoid the false peak caused by folding process in FFT calculation, we attached the low-pass filter corresponding to less than half of folding frequency. Sampling rate is usually 12.5MW/s, but sometimes 62.5MW/s was adopted in order to see more detail structure.

A. Argon

In Fig. 3, any voltage hash is not recognized. At $J=8.2$ kA, some degree of fluctuation occurs (Fig. 4). The narrow band frequency of 200 kHz is clearly recognized with additional random minute texture. At $J=11.2$ kA, the narrow band peak is shifted to higher frequency. Figures. 5- 7 were taken at completely same operational condition to confirm the repeatability of this experiment. In Fig. 8, we can see the narrow band peak is shifted to much higher point (700-800 kHz) at $J=13.7$ kA. The discharge current becomes larger, the amplitude of ΔV also becomes larger.

B. Hydrogen

As known well, some amount of voltage flucturation is always recognized in the wide range of discharge current. Figures. 9- 14 show this tendency. The narrow band peak is around 1 MHz, not so changed by the discharge current. The amplitude of the voltage fluctuation is also not so changed.

C. Xenon

At $J=6.6$ kA, the voltage waveform is very stable, but little a bit of increase of discharge current initiates the voltage fluctuation at $J=7.2$ kA. At this point, a frequency peak can be observed between 100 kHz and 200 kHz. At higher current, this peak becomes very ambiguous.

Table 3. Mass flow rate for each propellant used in the experiment.

propellant	\dot{m}
Ar	0.8g/s
Xe	1.5g/s
H ₂	0.7g/s

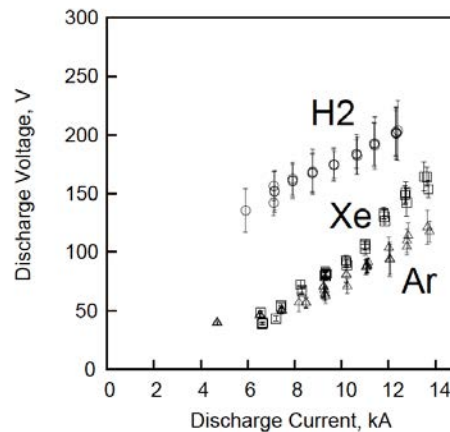


Figure 2. Discharge voltage vs. discharge current characteristics for various propellant.

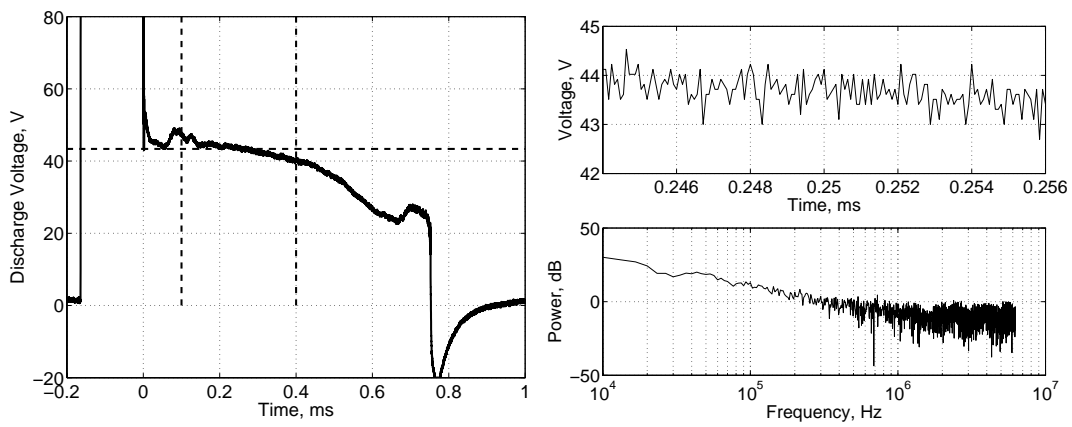


Figure 3. Discharge Voltage Waveform and its spectrum at $J= 4.6$ kA, $V = 43$ V with 0.8 g/s of argon

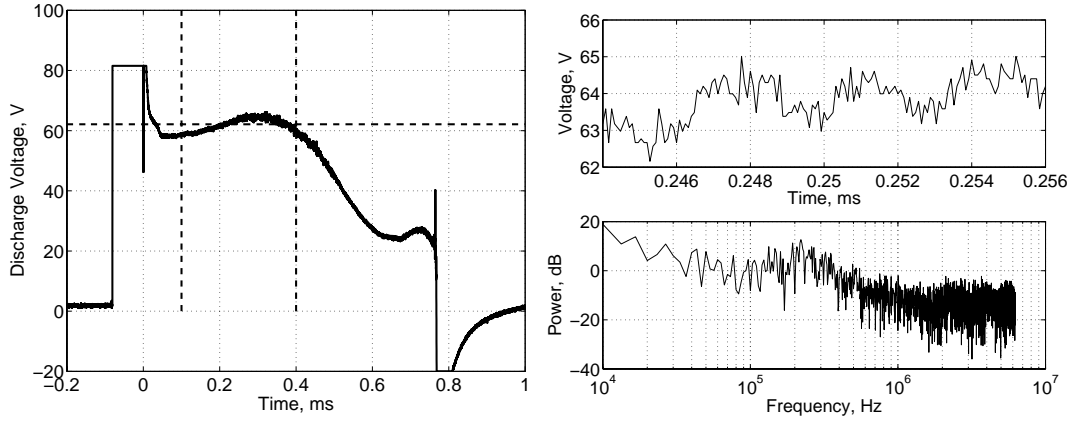


Figure 4. Discharge Voltage Waveform and its spectrum at $J= 8.2$ kA, $V = 62$ V with 0.8 g/s of argon

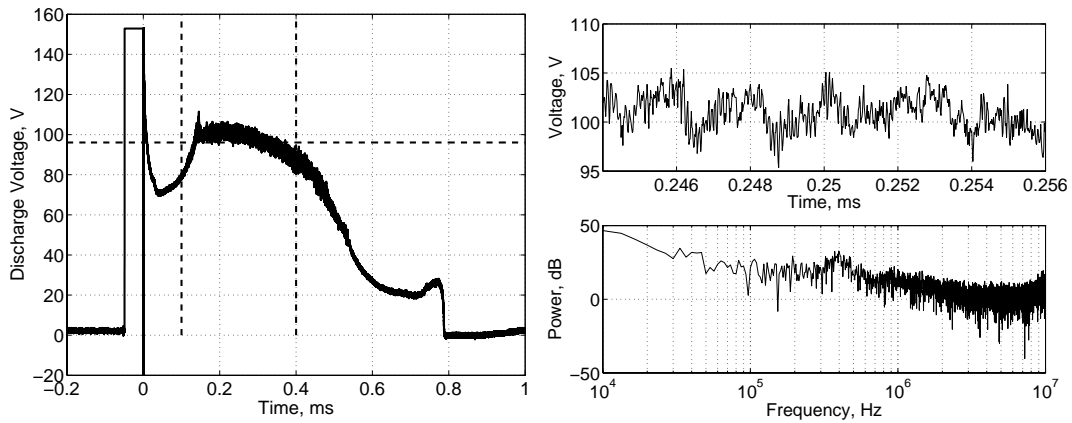


Figure 5. Discharge Voltage Waveform and its spectrum at $J= 11.1$ kA, $V = 96$ V with 0.8 g/s of argon

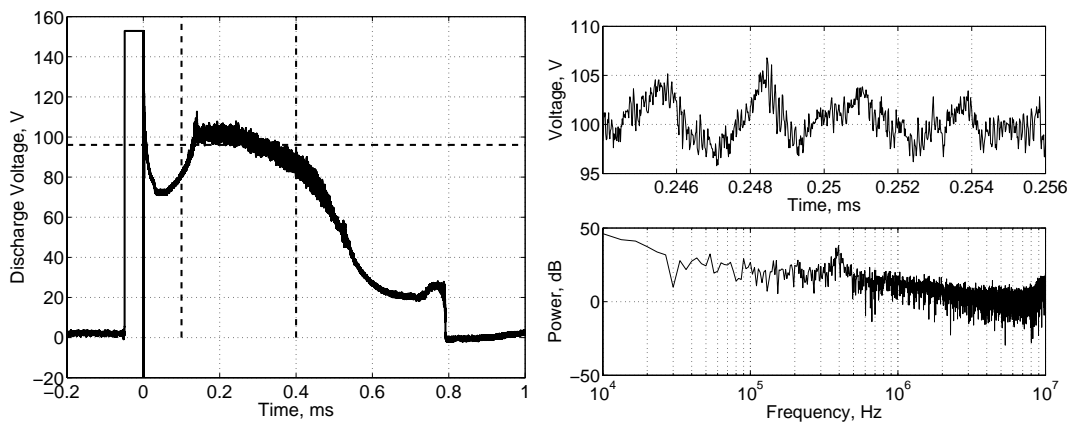


Figure 6. Discharge Voltage Waveform and its spectrum at $J= 11.0$ kA, $V = 96$ V with 0.8 g/s of argon

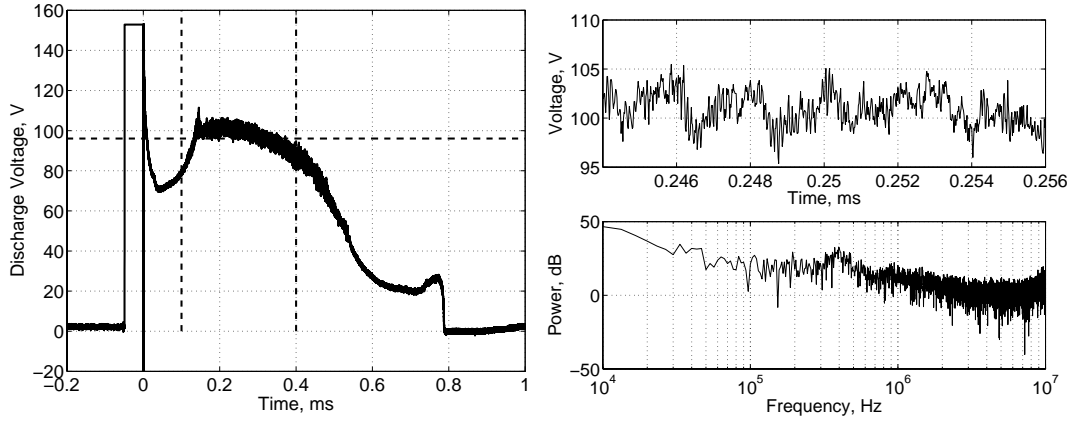


Figure 7. Discharge Voltage Waveform and its spectrum at $J= 11.1$ kA, $V = 95$ V with 0.8 g/s of argon

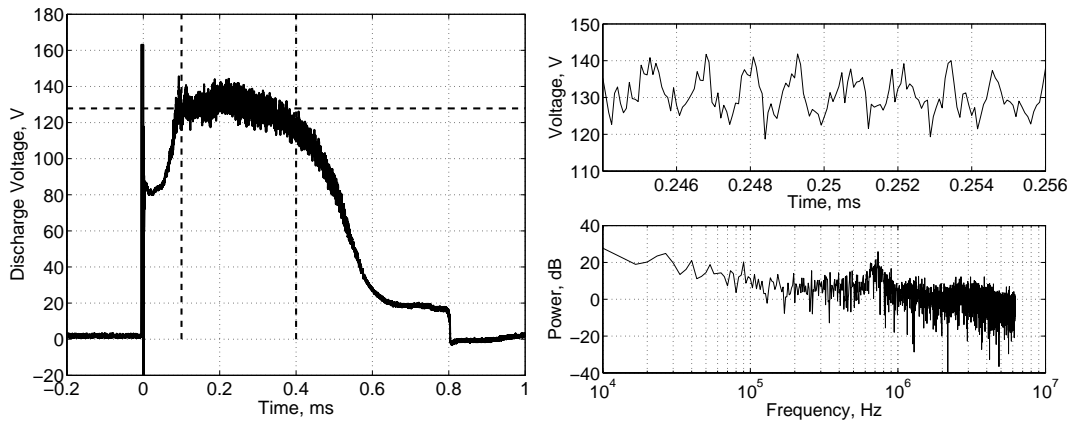


Figure 8. Discharge Voltage Waveform and its spectrum at $J= 13.7$ kA, $V = 128$ V with 0.8 g/s of argon

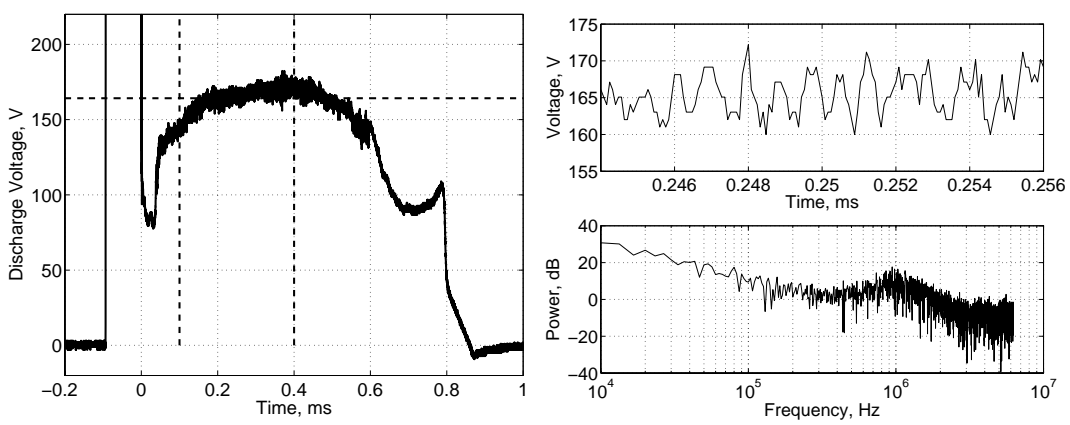


Figure 9. Discharge Voltage Waveform and its spectrum at $J= 7.1$ kA, $V = 164$ V with 0.7 g/s of hydrogen

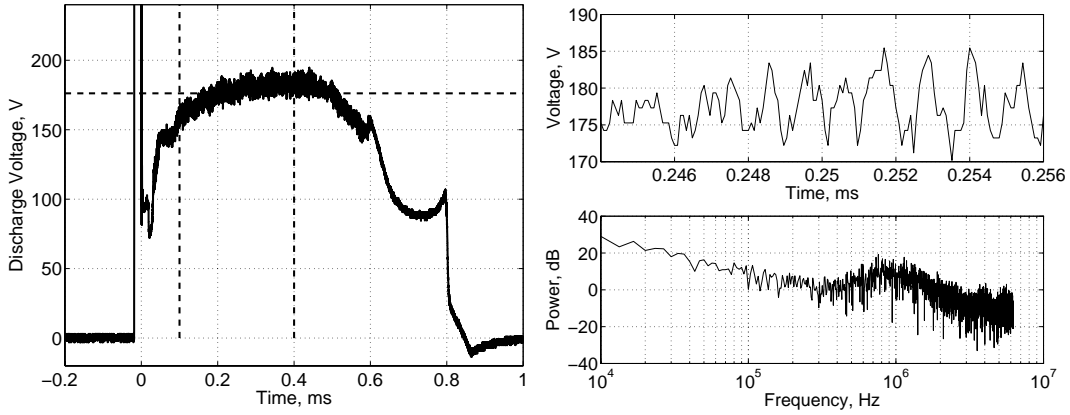


Figure 10. Discharge Voltage Waveform and its spectrum at $J= 8.8$ kA, $V = 176$ V with 0.7 g/s of hydrogen

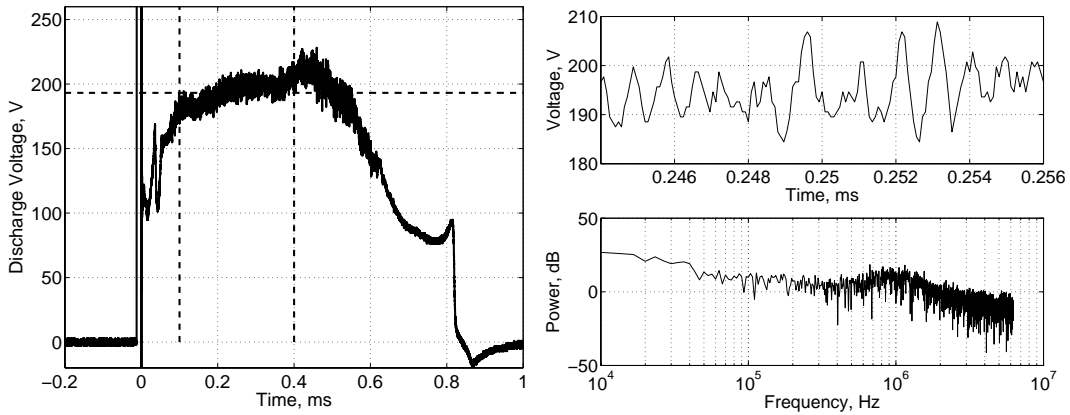


Figure 11. Discharge Voltage Waveform and its spectrum at $J= 10.6$ kA, $V = 193$ V with 0.7 g/s of hydrogen

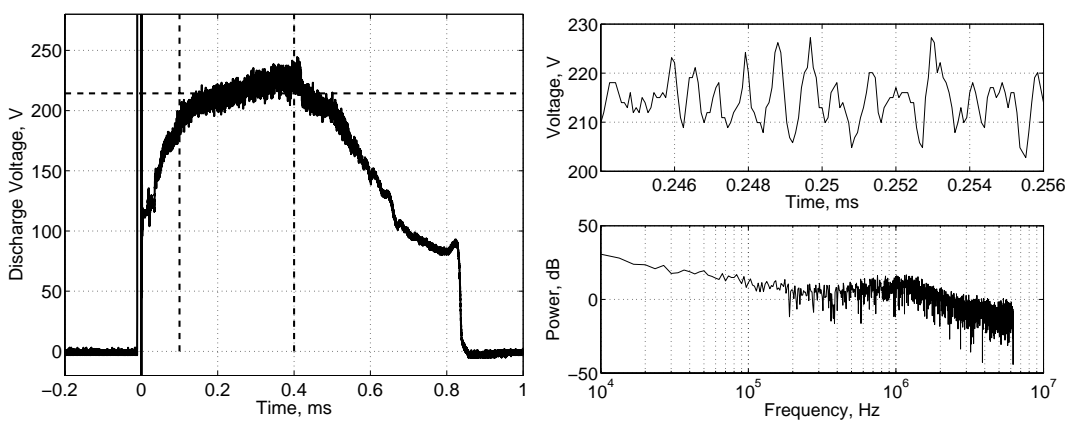


Figure 12. Discharge Voltage Waveform and its spectrum at $J = 12.3$ kA, $V = 214$ V with 0.7 g/s of hydrogen

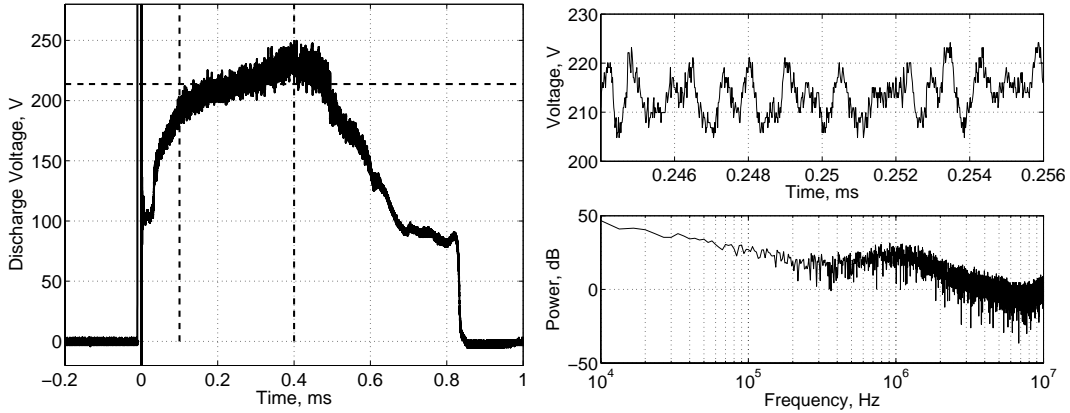


Figure 13. Discharge Voltage Waveform and its spectrum at $J = 12.3$ kA, $V = 214$ V with 0.7 g/s of hydrogen

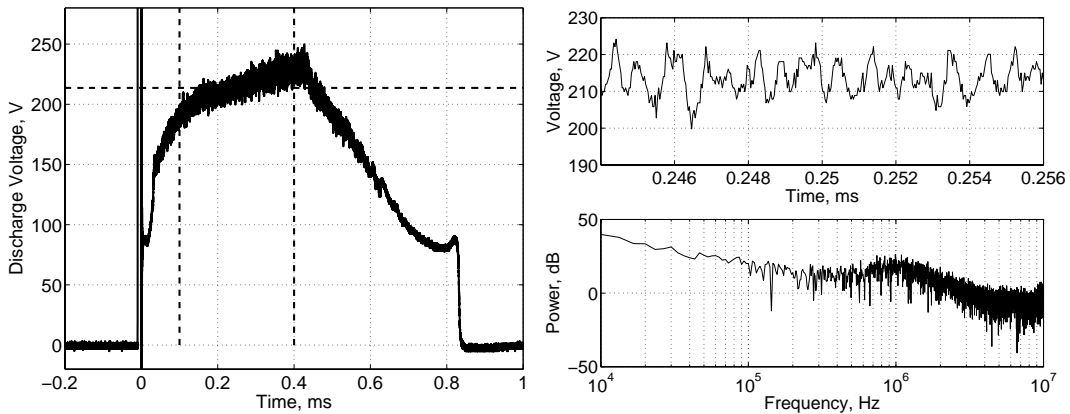


Figure 14. Discharge Voltage Waveform and its spectrum at $J = 12.3$ kA, $V = 214$ V with 0.7 g/s of hydrogen

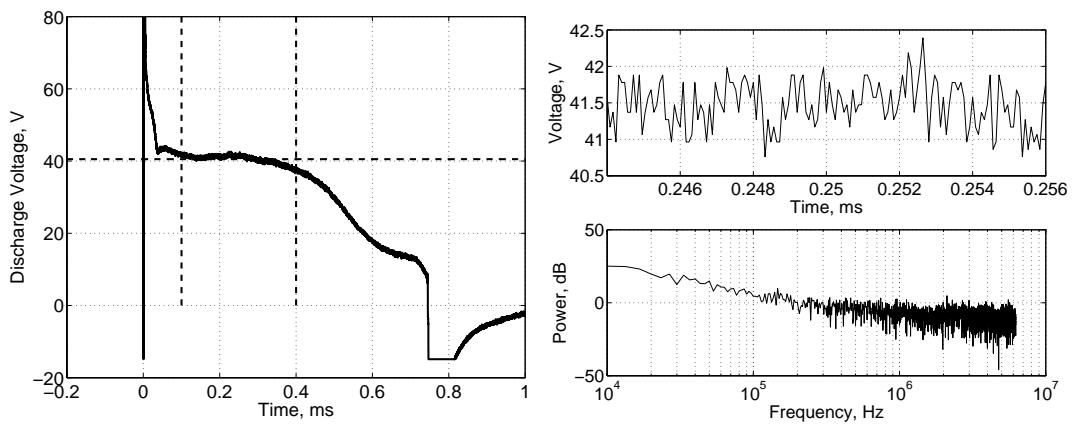


Figure 15. Discharge Voltage Waveform and its spectrum at $J = 6.6$ kA, $V = 40$ V with 1.5 g/s of xenon

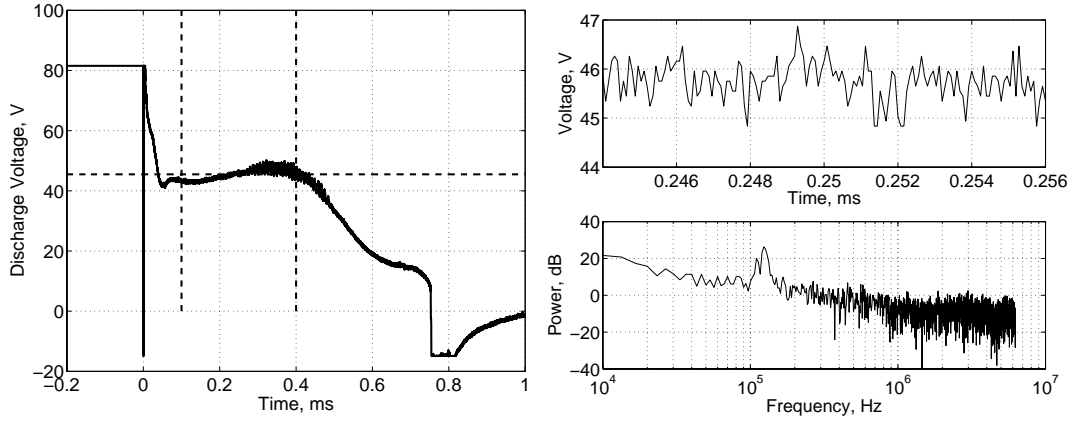


Figure 16. Discharge Voltage Waveform and its spectrum at $J = 7.2$ kA, $V = 45$ V with 1.5 g/s of xenon

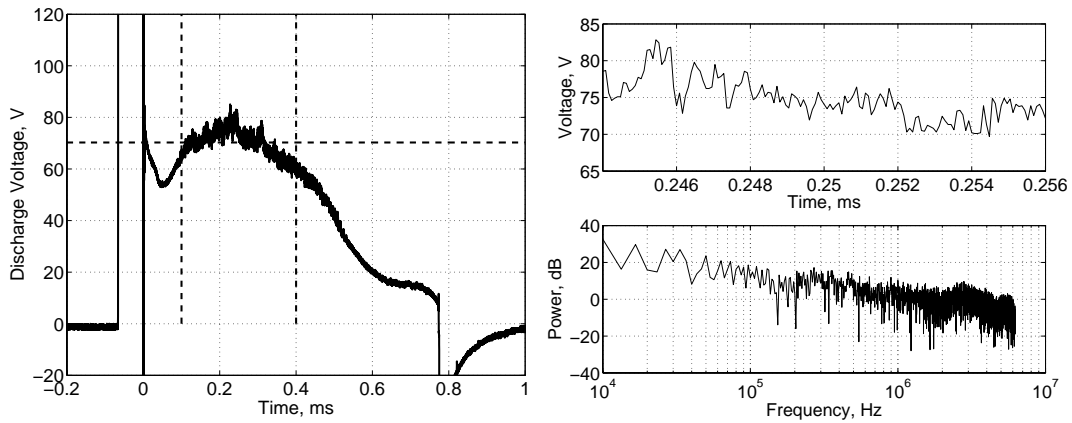


Figure 17. Discharge Voltage Waveform and its spectrum at $J = 8.3$ kA, $V = 70$ V with 1.5 g/s of xenon

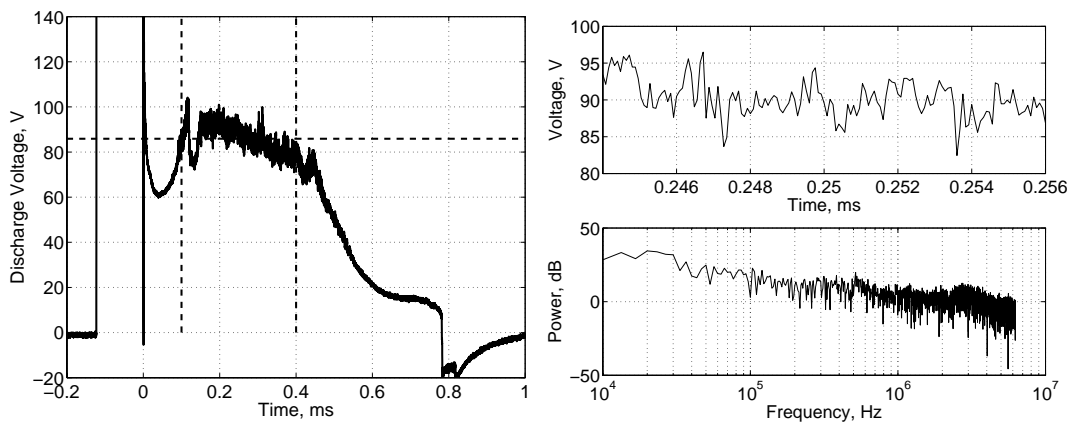


Figure 18. Discharge Voltage Waveform and its spectrum at $J= 9.3$ kA, $V = 86$ V with 1.5 g/s of xenon

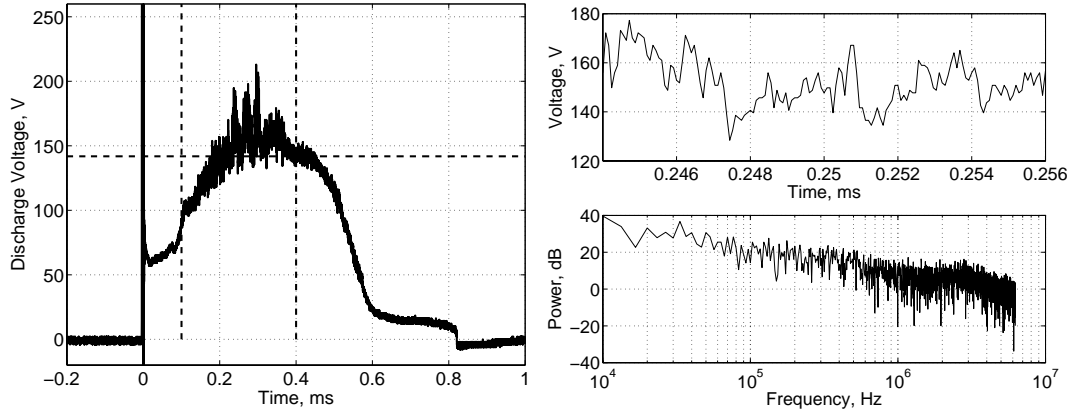


Figure 19. Discharge Voltage Waveform and its spectrum at $J= 12.8$ kA, $V = 142$ V with 1.5 g/s of xenon

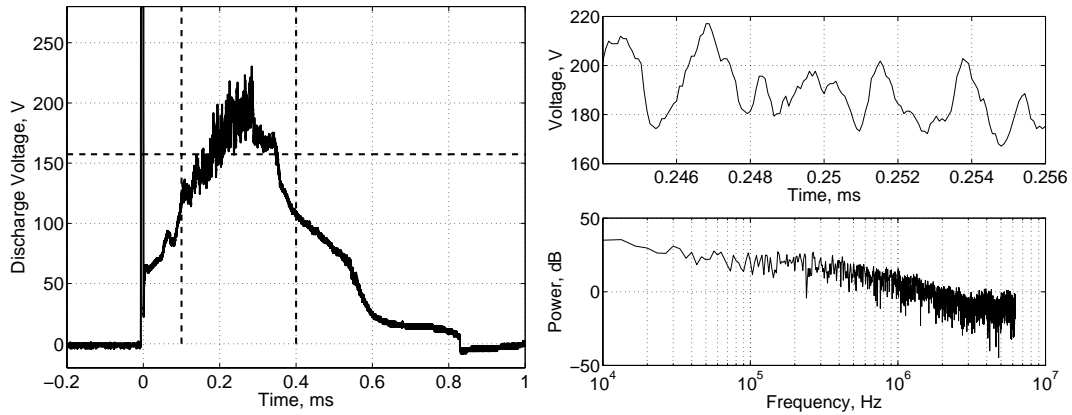


Figure 20. Discharge Voltage Waveform and its spectrum at $J= 13.5$ kA, $V = 157$ V with 1.5 g/s of xenon

IV. Discussion

A. The cause of voltage hash

Authors believe the "anode starvation theory" can explain the mechanism of voltage hash well, but it is still difficult question to explain the behavior of each propellant correctly. Hugel⁴ pointed out that the critical J^2/\dot{m} is almost inversely proportional to the molecular weight of the propellant from his experimental data although the raw voltage waveform was not displayed in his article. Argon, krypton and xenon were used in his experiment. Fischer² referred Hugel's explanation and mentioned that the cases of molecular propellant did not follow this tendency. Actually, in our experimental condition, 0.7 g/s of mass flow rate is very large value to achieve the starvation condition according to the $1/\sqrt{M}$ rule, but we can see the voltage fluctuation at any discharge current. One possible explanation for this problem is suggested by Michner and Kruger.⁸ They gave critical beta (β) instead of critical J^2/\dot{m} . In this theory, the dissociation energy of hydrogen also involves with the macroscopic fluctuation.

B. Is there a characteristic frequency in voltage hash ?

As shown in the previous section, we see narrow band peak frequency in many situation. Several hundreds of kHz spectrum is often reported^{9,10} in many literature, so it is sure that the lack of the electric career near the anode causes terminal voltage fluctuation following such a characteristic frequency. On the other hand, the theory that the voltage fluctuation is recognized as random noises.¹¹

In our experiment, we can see a random-noise situation in the case of xenon propellant at higher current. In this case, ΔV becomes very larger compared to the another propellant, finally reaches 40-50 V. Our simple conclusion here (just from the experimental observation) is that f_{peak} and ΔV becomes larger with increasing J^2/\dot{m} , and finally shows violent collapse. The situation explained by Uribarri¹¹ is corresponding to this situation. On the other hand, the transient situation where the f_{peak} is getting larger has been observed by Iida¹² in 1980s.

Here we cannot answer why the f_{peak} in case of hydrogen is almost constant at 1 MHz. If whole situation can be explained by "anode starvation theory", it has to be observed the fluctuation at lower current also causes severe anode erosion. If another mechanism causes the voltage fluctuation in lower J , This type of voltage hash is not a sign to show the threshold of an operational limit. In other words, this type of fluctuation is acceptable for practical use.

V. Conclusion

The behavior of the voltage fluctuation in an MPD thruster with argon, hydrogen and xenon propellants were examined, especially focusing on the relationship against the increasing discharge current. Following points were found in this experiment.

- For atomic gas (argon and xenon), the amplitude of the voltage fluctuation is getting larger with increasing current. The voltage fluctuation grew drastically especially in the case of xenon.
- For hydrogen, the amplitude of the voltage fluctuation is not so changed by the increase of discharge current. It is almost constant (= 10 V) in the wide range of discharge current.
- Certain level of narrow band peak is recognized for each propellant. In the case of argon, it varies from 200 kHz to 500 kHz with increasing current. For hydrogen, it is always constant (1 MHz) regardless of discharge current. For xenon, it is around 200 kHz at first, and becomes ambiguous at higher discharge current.

References

¹Choueiri, E. Y. and Ziemer, J. K., "Quasi-Steady Magnetoplasmadynamic Thruster Performance Database," *Journal of Propulsion and Power*, Vol. 17, No. 5, 2001, pp. 967-976.

²Fischer, E. and et al., "Self-Field MPD Thruster with Atomic and Molecular Propellants," *Appl. Phys. B*, Vol. 38, 1985, pp. 41-49.

³Uematsu, K., Morimoto, S., and Kuriki, K., "MPD Thruster Performance with Various Propellants," *Journal of Spacecraft and Rockets*, Vol. 22, No. 4, 1985, pp. 412-416.

- ⁴Hugel, H., "Effect of Self-Magnetic Forces on the Anode Mechanism of a High Current Discharge," *IEEE Transactions on Plasma Science*, Vol. PS-8, 1980, pp. 437-442.
- ⁵Funaki, I., Toki, K., and Kuriki, K., "Electrode Configuration Effect on the Performance of a Two-Dimensional Magnetoplasmdynamic Arcjet," *Journal of Propulsion and Power*, Vol. 14, No. 6, 1998, pp. 1043-1048.
- ⁶Nakata, D., Toki, K., Funaki, I., Shimizu, Y., Kuninaka, H., and Arakawa, Y., "Recent Study for Electrode Configuration and Material Improvement in an MPD Thruster," AIAA Paper 2007-5279, Jul. 2007.
- ⁷Uribarri, L. and Choueiri, E. Y., "Corruption of Pulsed Electric Thruster Voltage Fluctuation Measurements by Transmission Line Resonances," *Journal of Propulsion and Power*, Vol. 24, No. 3, 2008, pp. 637-639.
- ⁸Michner, M. and Jr., C. H. K., *Partially Ionized Gases*, John Wiley, New York, 1973.
- ⁹Kuriki, K. and Iida, H., "Spectrum Analysis of Instabilities in MPD Arcjet," IEPC 84-28, 1984.
- ¹⁰Uribarri, L. and Choueiri, E. Y., "Relationship Between Anode Spots and Onset Voltage Hash in Magnetoplasmdynamic Thrusters," *Journal of Propulsion and Power*, Vol. 24, No. 3, 2008, pp. 571-577.
- ¹¹Uribarri, L. and Choueiri, E. Y., "Creation of Onset Voltage Hash by Anode Spots in a Magnetoplasmdynamic Thruster," *Journal of Propulsion and Power*, Vol. 25, No. 4, 2009, pp. 949-957.
- ¹²Iida, H., "Instabilities in MPD Arcjet," Master Thesis in University of Tokyo, 1984.